Journal of Advanced Research (2015) 6, 405–415

Cairo University

Journal of Advanced Research

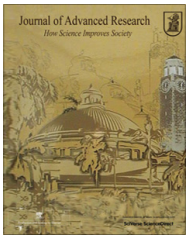

ORIGINAL ARTICLE

Individual and competitive adsorption of phenol and nickel onto multiwalled carbon nanotubes

Nour T. Abdel-Ghani [a,*], Ghadir A. El-Chaghaby [b], Farag S. Helal [c]

[a] *Chemistry Department, Faculty of Science, Cairo University, Giza, Egypt*
[b] *RCFF, Agricultural Research Center, Giza, Egypt*
[c] *Science & Technology Center of Excellence, Ministry of Military Production, Cairo, Egypt*

ARTICLE INFO

Article history:
Received 31 March 2014
Received in revised form 29 May 2014
Accepted 1 June 2014
Available online 6 June 2014

Keywords:
Adsorption
Carbon nanotubes
Nickel
Phenols
Equilibrium modeling

ABSTRACT

Individual and competitive adsorption studies were carried out to investigate the removal of phenol and nickel ions by adsorption onto multiwalled carbon nanotubes (MWCNTs). The carbon nanotubes were characterized by different techniques such as X-ray diffraction, scanning electron microscopy, thermal analysis and Fourier transformation infrared spectroscopy. The different experimental conditions affecting the adsorption process were investigated. Kinetics and equilibrium models were tested for fitting the adsorption experimental data. The characterization experimental results proved that the studied adsorbent possess different surface functional groups as well as typical morphological features. The batch experiments revealed that 300 min of contact time was enough to achieve equilibrium for the adsorption of both phenol and nickel at an initial adsorbate concentration of 25 mg/l, an adsorbent dosage of 5 g/l, and a solution pH of 7. The adsorption of phenol and nickel by MWCNTs followed the pseudo-second order kinetic model and the intraparticle diffusion model was quite good in describing the adsorption mechanism. The Langmuir equilibrium model fitted well the experimental data indicating the homogeneity of the adsorbent surface sites. The maximum Langmuir adsorption capacities were found to be 32.23 and 6.09 mg/g, for phenol and Ni ions, respectively. The removal efficiency of MWCNTs for nickel ions or phenol in real wastewater samples at the optimum conditions reached up to 60% and 70%, respectively.

Introduction

Industrial effluents contribute largely to environmental pollution problem. These effluents contain a variety of organic and inorganic pollutants. Among these pollutants phenol and nickel(II) are frequently encountered together in wastewaters such as from metal plating, dye and painting industries [1,2]. The maximum allowable concentration of nickel in effluents in the United States from the electroplating process wastewater is 4.1 mg/l [3] while that in drinking water should be less than 0.5 mg/l [4]. For phenol, the US Environmental Protection Agency (USEPA) regulations call for lowering its content in wastewater to less than 1 mg/l [5]. As per the World Health Organization regulation, the permissible limit for phenol concentration in potable water is 0.002 mg/l [6].

The presence of nickel ions and phenol in an aqueous environment causes a worldwide concern due to their toxicity

* Corresponding author. Tel.: +20 1006700375; fax: +20 235676501.
E-mail address: noureta2002@yahoo.com (N.T. Abdel-Ghani).

Peer review under responsibility of Cairo University.

Production and hosting by Elsevier

2090-1232 © 2014 Production and hosting by Elsevier B.V. on behalf of Cairo University.
http://dx.doi.org/10.1016/j.jare.2014.06.001

and carcinogenicity, which may result in damage to various systems of the human body [7].

Various conventional methods were designed and used to remove nickel ions and phenol from aqueous solutions such as adsorption, precipitation and coagulation, ion exchange, filtration, membrane separation, chemical oxidation, sedimentation, and reverse osmosis. Adsorption process is commonly applied because of its ease of application as well as its cost effectiveness [8].

In the recent years, carbon nanotubes have emerged as highly effective adsorbents for wastewater treatment. Carbon nanotubes (CNTs) discovered by Iijima in 1991 [9] are characterized by their unique structural, mechanical, chemical and physical properties [10]. The known ability of CNTs to establish π–π electrostatic interactions and their large surface areas can facilitate the adsorption of many kinds of pollutants from water [11]. CNTs have been proven to be superior adsorbent for removing many kinds of organic and inorganic pollutants [11,12]. CNTs display high distinctive surface areas and symbolize a new kind of adsorbent that offers a good option for removing various pollutants such as Ni(II) metallic ions [13] and phenol [14] from polluted water.

The objective of the present study was to investigate the adsorption capability of multiwalled carbon nanotubes (MWCNTs) for the removal of phenol and nickel ions from their individual and mixed aqueous solutions under different experimental conditions. The effects of contact time, initial pH, adsorbents loading weights, and initial nickel ions and phenol concentrations on the adsorption capacity of MWCNTs were investigated. The kinetics and equilibrium models of nickel and phenol adsorption onto MWCNTs were also studied.

Material and methods

Multiwalled carbon nanotubes

MWCNTs were purchased from Nanostructured & Amorphous Materials lnc. (820 Kristi Lane, Los Alamos, NM 87544, USA). The physical properties of the MWCNTs are listed in Table 1.

Chemicals

Analytical grade nickel nitrate (Merck Ltd., Taipei, Taiwan, 96–97% purity) and phenol (Fluka, 99.5%) were employed to prepare the stock solutions containing 1 g L^{-1} of Ni(II) and phenol, respectively. These stock solutions were further diluted using deionized water to the desired single or mixed nickel and phenol concentrations. HCl and NaOH used to adjust solutions pH were obtained from Sigma–Aldrich Company.

Table 1 Physical properties of MWCNTs.

Property	Value
Purity	>95%
Outside diameter	40–60 nm
Core diameter	5–10 nm
Length	5–15 μm
Specific Surface Area (SSA)	40–600 m^2 g^{-1}
Color	Black
Pore volume	0.8 cm^3 g^{-1}
Bulk density	~0.1 g cm^{-3}
True density	~2.1 g cm^{-3}

Adsorbent characterization

The adsorbent surface functional groups were determined by FTIR analysis, over the range of 500–4000 cm^{-1} with a resolution of 4 cm^{-1}using a Nicolet, AVATAR FTIR-370 Csl instrument. The microstructure of the adsorbent was examined using a Scanning electron microscopy (SEM, Quanta 250-FEI). The surface elemental composition analyses were proposed based on X-ray Powder Diffractometer (model ARL X′ TRA 156, Thermo Fisher Scientific Inc, USA. Thermogravimetric analysis of the adsorbent was also carried out using a thermogravimetric analyzer (TGA-Q500). pH was measured using pH meter (ORION model 420A) Thermo Scientific, USA.

Adsorption experiments

Batch adsorption studies were carried out at room temperature. The effect of contact time on phenol and nickel removal was investigated by mixing a known volume of phenol and/or nickel solution with a known adsorbent weight in stopped conical flasks for different time intervals (30–900 min). The solution-adsorbent mixtures were stirred at 100 rpm in a shaking water bath at 25 °C. At the end of each time interval the samples were filtered through Whatman No. 50 filter paper (2.7 μm size particle retention) to eliminate any fine particles. In all experiments blank measurements were taken.

The effect of each of the operational parameters affecting phenol and nickel ions adsorption was studied. Batch studies were performed as function of adsorbent dosage ranging from (0.2–1 g), solution pH (2–8) and adsorbate concentrations (5–100 mg/l) in separate experiments.

The concentration of phenol was determined using a double beam UV–vis spectrophotometer (Shimadzu UV-1601 Spectrophotometer, Japan) at 270 nm and nickel ions concentration was measured using an atomic absorption spectrometer (Shimadzu AA-6300) at 232 nm.

Phenol and nickel removal percentages were determined using equation

$$\text{Removal } \% = (C_i - C_f) \times 100/C_i \quad (1)$$

where C_i and C_f are the initial and final concentrations of phenol and nickel (mg/l) in the solution.

Adsorption capacity was calculated using equation

$$q = (C_i - C_f) \times (V/W) \quad (2)$$

where q is the adsorption capacity (mg g^{-1}), C_i is the initial adsorbate concentration in solution (mg/g), C_f is the equilibrium adsorbate concentration (mg/l), V is the volume of adsorbate solution (L) and W is the weight of the adsorbent (g).

The kinetics of phenol and nickel removal from aqueous solution by MWCNTs was studied by applying the pseudo-first-order [15] and pseudo-second-order [16] models. The adsorption mechanism was also investigated using the intra-particle diffusion model [17,18].

The equations describing the three studied models are presented by the following equations:

$$\ln(q_e - q_t) = \ln q_e - k_1 t \quad (3)$$

$$t/q_t = 1/k_2 q_e^2 + t/q \quad (4)$$

$$q_t = k_{(i)} t^{1/2} + C_{b(i)} \quad (5)$$

where q_e (mg g^{-1}) and q_t (mg g^{-1}) are the amounts of nickel ions (or phenol) adsorbed at equilibrium and at time (t), respectively, k_1 (min^{-1}) is the pseudo first order rate constant and k_2 (g mg^{-1} min^{-1}) is the rate constant of the second order equation. $k_{(i)}$ is the intra-particle diffusion parameter, and $C_{b(i)}$ is the thickness of the boundary layer at stage (i).

Adsorption isotherm studies were also carried out using the Langmuir [19] Eq. (6) and Freundlich [20] Eq. (7) isothermal models.

$$q_e = C_e/q_e = 1/bq_{max} + C_e/q_{max} \quad (6)$$

$$q_e = K_f C_e^{1/n} \quad (7)$$

where q_e and C_e represent the adsorbent capacity at equilibrium (mg g^{-1}) and the concentration of nickel (or phenol) at equilibrium (mg/l), respectively. In the Langmuir equation, q_{max} is considered the maximum sorption capacity related to the total cover of the surface and b is associated with sorption energy. From the Freundlich model, K_f represents the sorption capacity and $1/n$ is related to the energy distribution of the sorption sites.

Competitive adsorption studies

Following the procedure given by Tang et al. [21]; the competitive adsorption experiments were performed when both adsorbates were adsorbed onto MWCNTs simultaneously. In the competitive adsorption studies, the concentration of Ni(II) and phenol in their mixed solution was varied between 25 and 100 mg/l (for both adsorbates). The competitive studies were performed at the optimum previously achieved operating conditions.

Results and discussion

Characterization

Generally, the adsorption ability of MWCNTs was known to be attributed to its surface chemical composition and rich surface area [22]. Fig. 1 shows the X-ray diffraction patterns of raw MWCNTs.

From Fig. 1 it can be seen that the diffractogram of raw MWCNTs exhibits the typical peaks at 2θ around 26.5° and 42.7°, corresponding to the normal structure of graphite (002) and (100) reflections (Joint Committee for Powder Diffraction Studies (JCPDS) No. 01-0646) respectively [22]. Similar findings were reported by Chen et al. [23], Gupta et al. [24], Oh et al. [25] and Chen & Oh [26].

Scanning electron microscopy (SEM) imaging was also used to characterize the surface morphology of multiwalled carbon nanotubes. Fig. 2 displays the SEM images of raw MWCNTs. It is evident from the figure that the MWCNTs are cylindrical in shape, curved and tangled together [18,27]. The length of the raw MWCNTs is in the range of 5–15 μm.

TG–DTG analysis of the MWCNTs was obtained by heating the samples from 30 to 900 °C at a ramping rate of 10 °C/min under nitrogen gas atmosphere. TGA analysis was performed to estimate the homogeneity of the raw MWCNTs and its thermal stability [27].

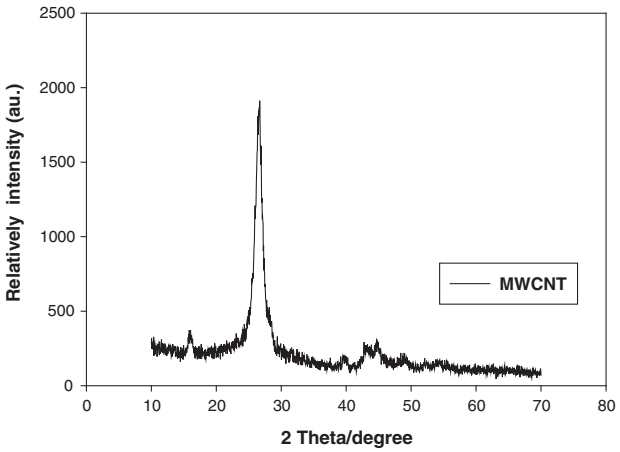

Fig. 1 XRD patterns of raw MWCNTs.

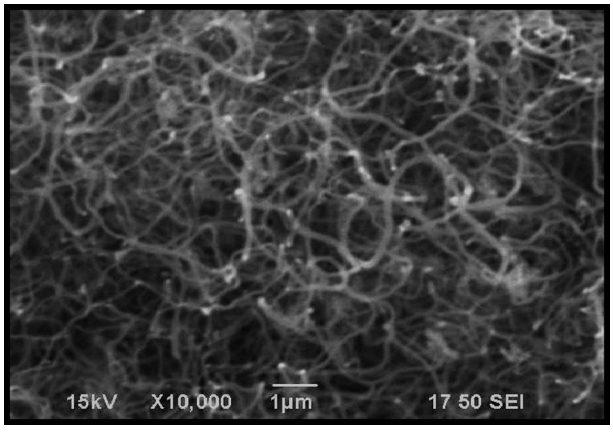

Fig. 2 Scanning electron microscopy (SEM) image of raw MWCNTs (10000×).

Fig. 3 displays the TGA results of raw MWCNTs. It is evident that MWCNTs are considerably stable and show a little weight loss close to 4.37% below 550 °C. Then MWCNTs decomposed in one stage until they are completely decomposed around 720 °C [18,21,27]. The obvious weight loss over the range of 550–720 °C was caused by the oxidization of the nanotubes [28].

Fig. 4 presents the FTIR spectra of (a) raw MWCNTs, (b) phenol-loaded MWCNTs, (c) Ni(II)-loaded MWCNTs and (d) phenol and Ni(II)-loaded MWCNTs. As seen from Fig. 4(a), the spectra of raw MWCNTs exhibit a broad absorption band at around 3423 cm^{-1} corresponding to (—OH) stretching vibration of the surface hydroxyl groups [24,29]. The two observed peaks at 2924 and 2855 cm^{-1} are somewhat weak and could be attributed to SP3 (C—H) stretching vibration motions [30], originated from the surface of tubes [24] or of the sidewalls [31].

The small band at around 1650 cm^{-1} could be attributed to the presence of COO, C=O stretching mode of functional groups on the surface of raw MWCNTs and can also indicate the bending vibration of adsorbed water or arising from the

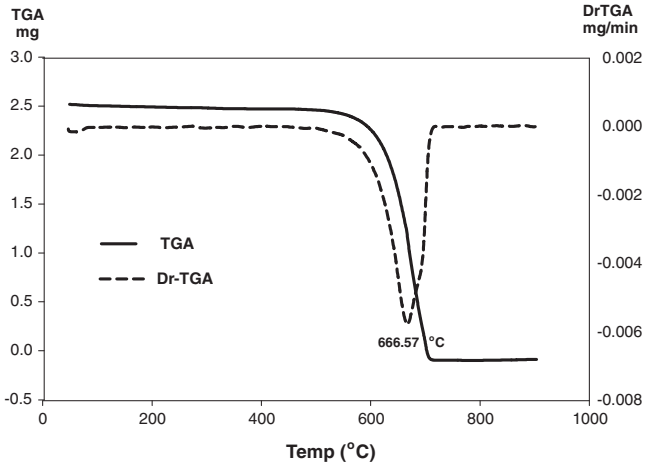

Fig. 3 TG–DTG curves of raw MWCNTs.

absorption of atmospheric CO_2 on the surface of MWCNTs [24]. The peaks between ~1000 and 1380 cm^{-1} can be attributed to C—O stretching of COOH and —OH bending modes of alcoholic, phenolic and carboxylic groups [29]. In addition, sharp band at ~1380 cm^{-1} confirmed the existence of a C—O bond on raw MWCNTs, reinforcing the interaction with carboxylate groups [22].

The changes in the surface functional groups of raw MWCNTs after adsorption of phenol and nickel ions were also confirmed by FTIR spectra through the changes in the positions of some the peaks as well as the appearance of some new peaks.

The stretching band of C=C at 1420 cm^{-1} on raw MWCNTs got split into 1419 and 1461 cm^{-1} when both phenol and nickel ions were individually adsorbed and was shifted to 1456 cm^{-1} when they were simultaneously adsorbed.

Fig. 4(b–d) displays new peaks in the range of around 2340–2360 cm^{-1} that were absent in the spectra of raw MWCNTs. These peaks can be related to —OH stretch

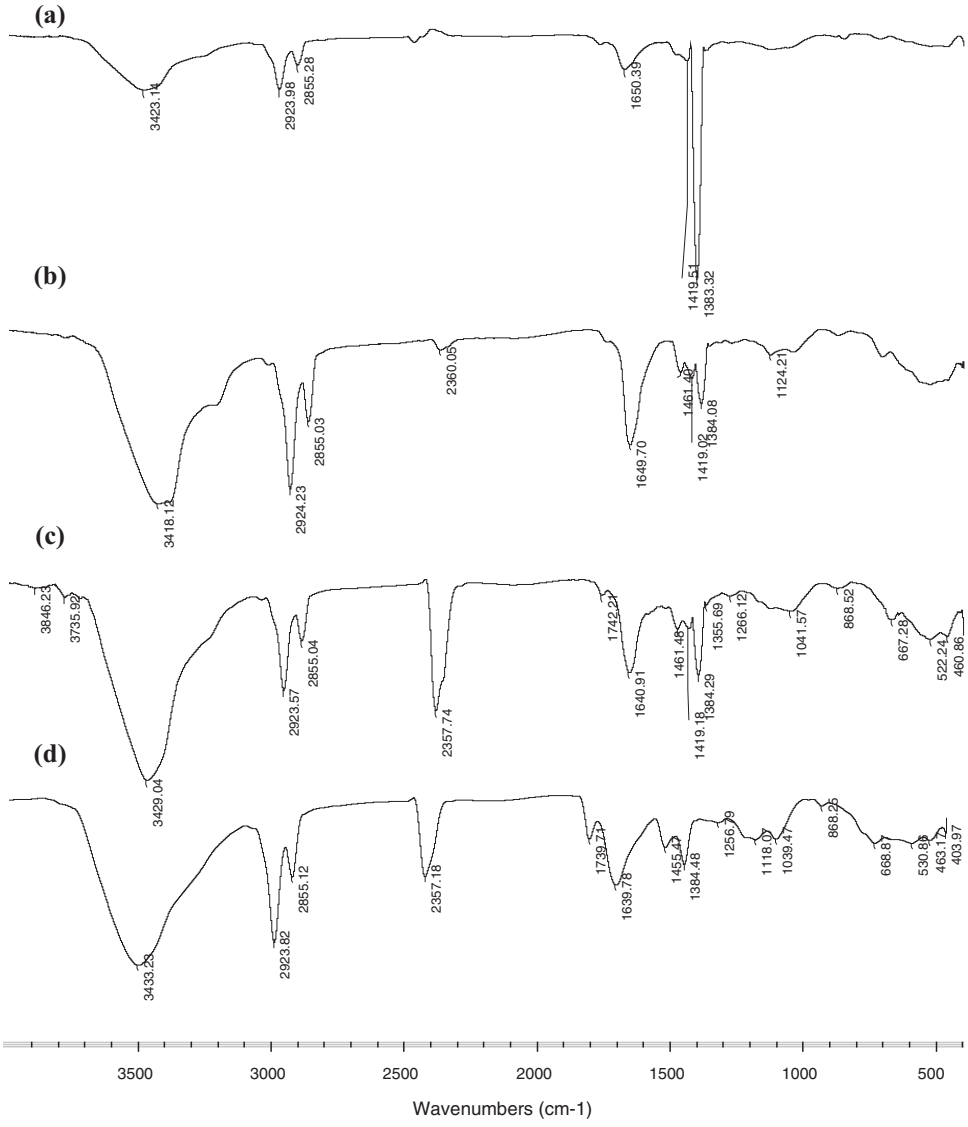

Fig. 4 FTIR spectra of (a) raw MWCNTs, (b) phenol-adsorbed MWCNTs, (c) Ni(II)-adsorbed MWCNTs and (d) phenol and Ni(II)-adsorbed MWCNTs.

from strong H—bonded—COOH [30]. These peaks at 2340–2360 cm^{-1} could also be assigned to CO_2 that was absorbed during the realization of the FTIR spectra.

The emerging peaks at wave numbers 1742 and 1740 cm^{-1} are associated with C=O (carbonyl groups) stretching mode of carboxylic acid in case the Ni(II) is adsorbed alone or together with phenol, respectively [22].

The new peaks around 400–870 cm^{-1} in case of Ni(II)-adsorbed MWCNTs and phenol and Ni(II)-adsorbed MWCNTs were assigned to the strong bonding between the metal ions and the nanotube through oxygen-containing functional groups [32]. The new absorption peaks at ~400–870 cm^{-1} in Fig. 4(c and d) were attributed to Ni—O stretch, suggesting the formation of nickel oxides on the surface of MWCNTs.

FTIR spectra showed that raw MWCNTs are mainly composed of polymeric OH groups, CH_2 and COO groups. According to Machado et al. [33] these functional groups (OH, COOH, C—O, etc.) played an important role in adsorption due to their electrochemical properties. These oxygen-containing functional groups can provide numerous adsorption sites and thus increase the adsorption capacity for phenol molecules and nickel ions [29].

Effect of contact time and adsorption kinetics

The effect of contact time on the removal percentage of phenol and Ni(II) by adsorption onto MWCNTs was studied at different time intervals (from 30 to 900 min) at room temperature (Fig. 5). The other experimental factors were kept constant at an initial phenol and Ni(II) concentration of 25 mg/l, an adsorbent dosage of 5 g/l, and at a solution pH = 7. The results showed that the removal of both adsorbates increased gradually until equilibrium was reached after 300 min. Thus this contact time was used in subsequent experiments.

The adsorption kinetic data of phenol and nickel ions onto MWCNTs were analyzed using three different kinetic models: the Lagergren pseudo-first-order model [15], the pseudo-second-order model [16] and Weber and Morris intra-particle diffusion model [17,18] represented by Eqs. (3)–(5); respectively.

The linear plots of log ($q_e - q_t$) versus t for different concentrations of nickel ions (or phenol) are shown in Fig. 6. The obtained values of k_1, calculated q_e values and determination

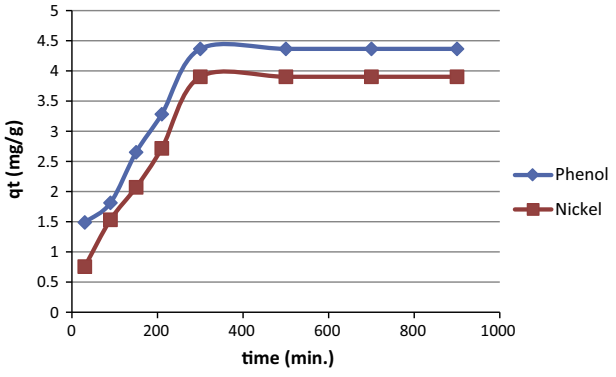

Fig. 5 Effect of contact time on phenol and nickel removal by MWCNTs (initial phenol and Ni(II) concentration of 25 mg/l, adsorbent dosage 5 g/l, and solution pH 7).

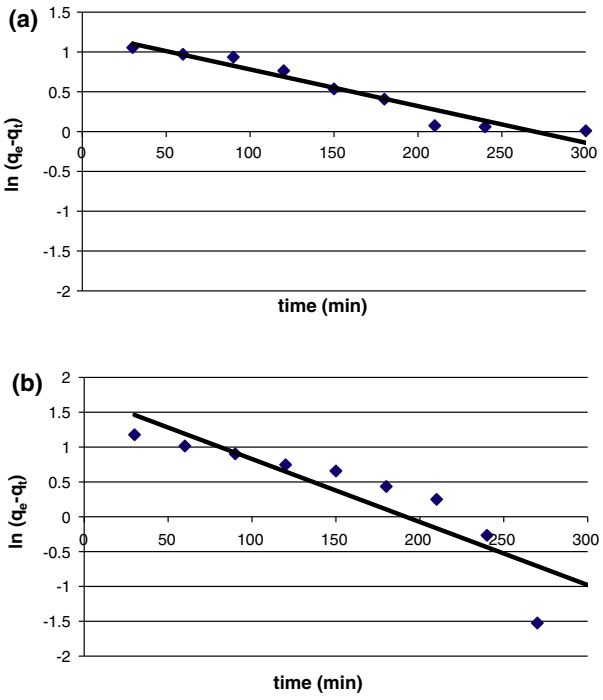

Fig. 6 Lagergren first order kinetics for the adsorption of (a) phenol and (b) Ni(II) onto MWCNTs.

coefficients R^2 for adsorption of nickel ions (or phenol) on MWCNTs are given in Table 2.

The Lagergren model's R^2 value for adsorption of phenol was found to be relatively high >0.94 and the experimental q_e value was found to be in good agreement with that calculated q_e value obtained from the linear Lagergren plots.

These results may be used as indication for the applicability of Lagergren equation to phenol adsorption on MWCNTs. Thus it can be concluded that the adsorption of phenol on MWCNTs follows the Lagergren first order kinetics and the process depends on both the solution concentration and the number of available adsorption sites [34].

On the other hand, the line obtained for adsorption of Ni(II) showed a poor fitting with relatively low R^2 value ($\leqslant$0.81) and notable variances between the experimental and theoretical amount of nickel ions. The obtained results indicate that the pseudo-first-order equation was not appropriate for describing the adsorption of the target nickel ions by MWCNTs.

In many adsorption processes, the Lagergren pseudo-first-order equation did not fit well the whole range of contact time and was generally applicable over the initial stage (20–30 min) of the adsorption processes [35]. Kinetic data were further treated with the pseudo-second-order kinetic model [36].

For many adsorbate–adsorbent systems, where both physical and chemical adsorption occurs, the adsorption data are well correlated by the pseudo-second-order equation [37]. The integral form of the model represented by Eq. (4)predicts that the ratio of the time/adsorbed amount should be a linear function of time [38].

By applying the pseudo-second-order rate equation to the experimental data for the adsorption of phenol and Ni(II) Fig. 7 was obtained.

Table 2 The first-order, second-order and kinetic models' constants for phenol and nickel ions adsorption by MWCNTs.

Adsorbate	First-order kinetic model				Pseudo-second-order model				q_e Experimental (mg/g)
	k_1 (min^{-1})	$q_{calc.}$ (mg/g)	R^2	Δq	k_2 (g/mg min)	$q_{calc.}$ (mg/g)	R^2	Δq	
Phenol	0.005	3.72	0.939	0.640	3.03×10^{-3}	4.10	0.994	0.26	4.36
Ni(II)	0.01	7.41	0.805	−3.290	5.5×10^{-5}	4.29	0.963	0.17	4.12

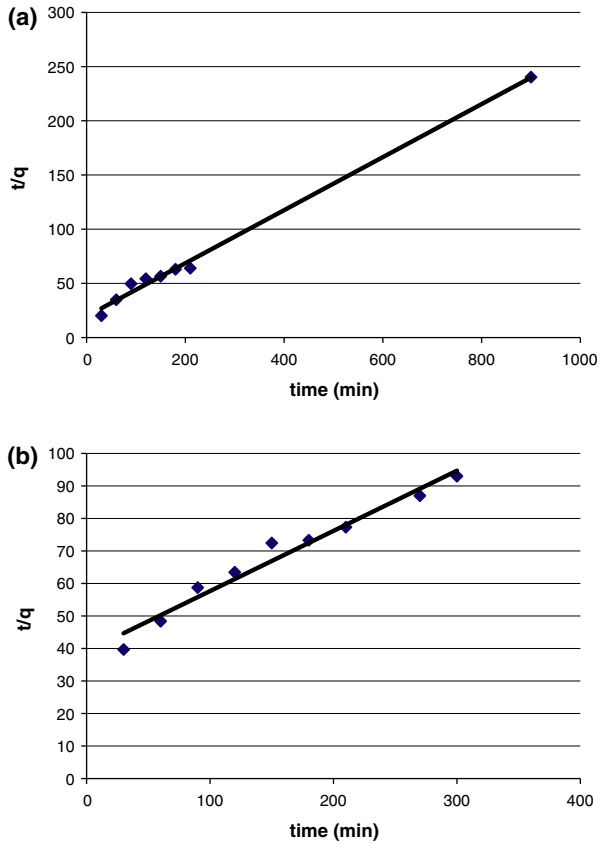

Fig. 7 Pseudo-second order kinetics for the adsorption of (a) phenol and (b) Ni(II) onto MWCNTs.

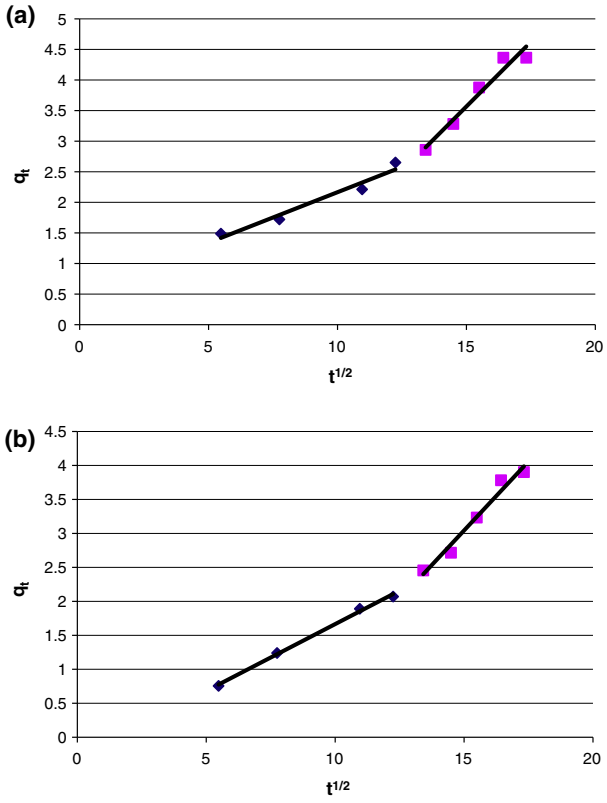

Fig. 8 Intra-particle diffusion mechanism for the adsorption of (a) phenol and (b) Ni (II) onto MWCNTs.

The pseudo-second-order rate equation parameters calculated from the slope and intercept of the plot of (t/q_t) vs. (t) are presented in Table 2. It is clear from the data that all of the experimental data had good determination coefficient values (R^2), which indicates the suitability of the pseudo-second-order rate equation for the description of the adsorption of the target metal ions and phenol from aqueous solutions by MWCNTs.

The amounts of phenol and nickel ions adsorbed per unit mass of MWCNTs at equilibrium (q_e), calculated from the slope of the plot of t/q_t vs. t, were in good agreement with experimental values. The above results suggested that the pseudo-second order adsorption mechanism was prevalent for the adsorption phenol and Ni(II) by MWCNTs [36,39].

Also, according to Wu et al. [40] the pseudo-second-order model was suitable for the adsorption of low molecular weight adsorbates on smaller adsorbent particles, which could explain for its applicability in this study. The suitability of the pseudo-second-order rate equation for the adsorption of phenol and Ni(II) by MWCNTs agreed well with many previous studies [18,41].

The similar phenomena have also been observed in the adsorption of phenol on activated carbons prepared from beet pulp [42], plum kernels [43] and rattan sawdust [44]. Also, the pseudo-second-order rate equation was reported to fit the kinetics of Ni(II) sorption onto sphagnum moss peat [39], Azadirachta indica (leaf powder) [45] and meranti sawdust [46].

The mechanism by which phenol and Ni(II) are adsorbed from aqueous solutions by MWCNTs was investigated using the intra-particle diffusion model. Since neither the pseudo first-order nor the pseudo-second-order kinetic models can identify the diffusion mechanism, the kinetic results were then analyzed by using the intra-particle diffusion model to determine the diffusion mechanism. A Plot between (q_t) versus $(t^{1/2})$ representing the intra-particle diffusion model is given in Fig. 8.

The values of $k_{(i)}$ and $C_{b(i)}$ can be calculated from the slope and intercept, respectively, and the results are tabulated in Table 3. From Table 3 it can be observed that high determination coefficient values ($R^2 > 0.95$) were obtained for the intra-particle diffusion model suggesting the applicability of the model for describing the adsorption of phenol and Ni(II) onto MWCNTs.

Table 3 Intra-particle diffusion mechanism constants for phenol and nickel adsorption by MWCNTs.

Adsorbate	Intra-particle diffusion					
	k_1 (mg/g min$^{1/2}$)	$C_{b(1)}$ (mg/g)	R^2	k_2 (mg/g min$^{1/2}$)	$C_{b(2)}$ (mg/g)	R^2
Phenol	0.1652	0.5137	0.9560	0.4226	2.7709	0.9968
Ni(II)	0.1968	0.3026	0.9510	0.4063	3.0516	0.9695

As seen from Fig. 8, multi-linear plots with two linear portions were obtained for the adsorption of phenol and Ni(II) from aqueous solution onto MWCNTs. The initial or first stage may be attributed to the effect of boundary layer (external mass transfer) diffusion, i.e. surface adsorption while the second stage may also be due to intra-particle diffusion effects [47].

The nonzero intercepts of the plots in each case were a clear indication that the rate-controlling process is not only due to the intra-particle diffusion some other mechanism along with intra-particle diffusion is also involved in the adsorption process [48].

Effect of pH

The solution pH affects both the surface charge of the adsorbent and the degree of ionization and speciation of the adsorbate [8]. In the present study the pH was varied between of 2 to 8 and higher pH values were omitted to avoid hydroxide precipitation of nickel ions. The other experimental parameters were kept constant e.g. contact time (300 min), adsorbent dosage (5 g/l) and adsorbate concentration (25 mg/l).

Fig. 9 illustrates the effect of solution pH on the removal of nickel ions and phenol from their solutions. It was found that the removal percentage of Ni(II) increased as the solution pH increased due to the increase in the electrostatic attractive forces between OH− and Ni^{2+} [8].

According to Chen et al. [23] as pH increases, the adsorbent functional groups are progressively deprotonated, forming negative oxidized MWCNTs charge. The attractive forces between the anionic surface sites and cationic metal ions easily result in the formation of metal–ligand complexes.

It is known that divalent metal ions (M^{2+}) can be present in deionized water in the forms of M^{2+}, $M(OH)^{+1}$, $M(OH)2^{0}$, $M(OH)3^{-1}$, etc. [11,13]. At a pH $\leqslant$ 8, the predominant nickel species is always Ni^{2+}. Thus, the fact that more Ni^{2+} sorption took place at a higher pH could be attributed to a decrease in competition between H^+ and Ni^{2+} at the same sorption site of MWCNTs. Furthermore, the surface of MWCNTs is more negatively charged at a higher pH, which causes a more electrostatic attraction of Ni^{2+}.

From Fig. 9 it can be also noticed that the removal of phenol by MWCNTs increased by increasing the solution pH from 2 to 7 and decreased thereafter. At pH 7 the maximum removal of phenol by MWCNTs, was found to be approximately 87.5%. The dependence of phenol removal on the solution pH could be explained in term of both the adsorbent surface charge and the adsorbate species present in solution.

From Fig. 10 it can be concluded that the MWCNTs have a pH_{PZC} equal to 6 and the adsorbent surface charge is positive at pH < 6 whereas at pH > 6 the surface charge is negative. On the other hand the pK_a value of phenol is 9.99 hence below this pH phenol is considered a neutral molecule and above this value is found as anionic species [14]. Thus at low pH values the surface charge is positive and the H^+ ion concentration in solution is high, therefore competition between H^+ and phenol species could occur [14] which cause a low adsorption of phenol by MWCNTs. At pH 7 where the maximum phenol removal was achieved, the adsorbent surface is negatively charged and neutral phenol species are present in solution. Therefore, there is no repulsion between phenol and the adsorbent, and their interaction can happen in a free way through π electrons [14].

Based on the above results, pH value of 7 was kept constant in the subsequent experiments to ensure maximum removal of both phenol and nickel ions.

Equilibrium modeling

Equilibrium study on adsorption provides information on the adsorbent capacity. In the present study, Langmuir and Freundlich sorption isotherm models were used to determine

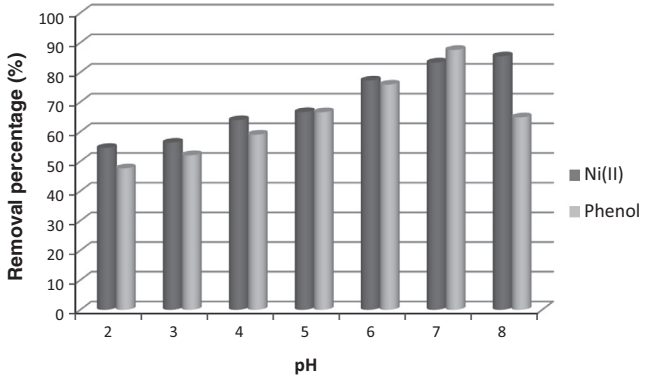

Fig. 9 Effect of pH on the adsorption of Ni (II) and phenol by MWCNT [contact time (300 min.), adsorbent dosage (5 g/l) and adsorbate concentration (25 mg/l)].

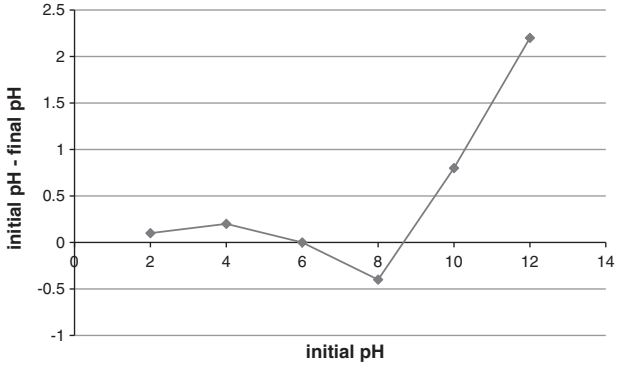

Fig. 10 Point of zero charge pH_{pzc} of MWCNTs.

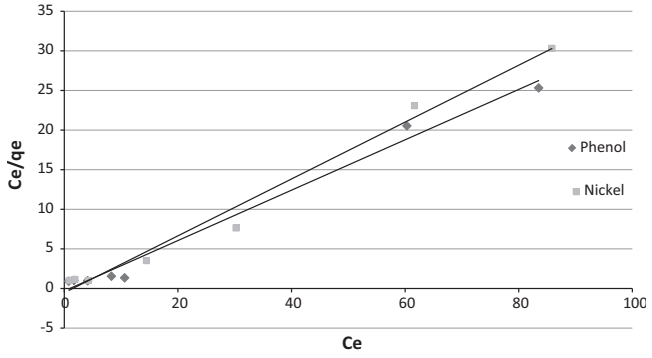

Fig. 11 Langmuir isotherm for the adsorption of phenol and Ni(II) onto MWCNTs (pH:7; biomass weight: 0.25 g/50 mL; shaking speed: 100 rpm; temp.: 25 °C).

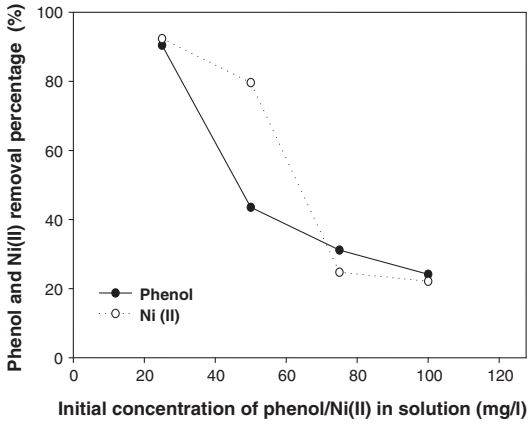

Fig. 13 Simultaneous adsorption of phenol and Ni(II) by MWCNTs.

the model that best fits the experimental data of nickel and phenol adsorption onto MWCNTs.

The constants of the Langmuir and Freundlich models for nickel and phenol adsorption onto MWCNTs were obtained from the plots presented in Figs. 11 and 12 and their values are summarized in Table 4. It was observed that the Langmuir isotherm better described the adsorption of phenol with the higher determination coefficient R^2 close to 1 (0.990), suggesting that homogeneous sorption on the surfaces of MWCNTs occurred. These results were consistent with many previous works where the Langmuir isotherm was more suitable than the Freundlich isotherm for the adsorption of phenol on various adsorbent, as activated carbons [49], dried aerobic activated sludge [1], Schizophyllum commune fungus [50], activated carbon prepared from biomass material [44] and activated carbon produced from avocado kernel seeds [51].

Also, adsorption data for Ni(II) were better fitted with the Langmuir isotherm (0.983), from which it could be assumed that the adsorbed Ni(II) formed monolayer coverage on the adsorbent surface and all adsorption sites were equal with uniform adsorption energies without any interaction between the adsorbed molecules. Similar results have also been observed by earlier researchers [23,29].

The value of constant b, which is related to free energy of sorption, in the Langmuir isotherm played an important role to simulate the concentration at which the phenol amount is bound and indicates the affinity for the binding of phenol. A high b value indicates a high affinity [1]. The b values of phenol and Ni(II) are 3.17 and 2.82 (L mg−1), respectively, which indicates that the bonding of phenol on MWCNTs is much stronger than that of Ni(II).

Simultaneous adsorption between phenol and Ni(II)

Competitive adsorption of phenol and Ni(II) was evaluated when both adsorbates were adsorbed simultaneously on MWCNTs (Fig. 13).

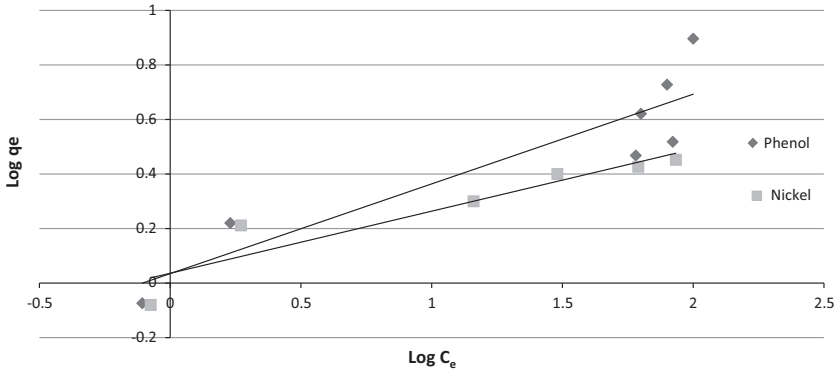

Fig. 12 Freundlich isotherm for the adsorption of phenol and Ni(II) onto MWCNTs (pH:7; biomass weight: 0.25 g/50 mL; shaking speed: 100 rpm; temp.: 25 °C).

Table 4 Langmuir and Freundlich parameters for phenol and Ni(II) adsorption by MWCNTs.

Adsorbate	Langmuir model			Freundlich model		
	q_{max} (mg g^{-1})	b (L mg^{-1})	R^2	K_f	n	R^2
Phenol	32.25	3.17	0.990	1.11	1.76	0.896
Ni (II)	6.09	2.82	0.983	1.07	4.48	0.871

Table 5 Maximum sorption capacities of phenol and nickel ions with MWCNTs and other sorbents.

Sorbents	Maximum sorption capacities (q_{max}) (mg g^{-1})		References
	Phenol	Ni (II)	
MWCNTs	32.25	6.09	Present work
MWCNTs	15.90	—	[53]
PHEMA microbead modified Cibacron blue	8.30	—	[54]
PHEMA microbead modified alkali blue 6B	13.60	—	[55]
Samla coal	13.30	—	[56]
Natural coal	18.80	—	[57]
Activated coal	1.48	—	[58]
Kaolinite	—	1.67	[59]
Chitosan	—	2.40	[60]
Chabazite	—	4.50	[61]
Chabazite–phillipsite	—	0.56	[62]
Activated carbon (AC) cloths: CS 1501	—	5.80	[63]
Grapefruit peel		46.13	[64]
Treated algae		40.9	[65]

The results showed that increasing the concentration of nickel from 25 mg/l to 50 mg/l resulted in about 51% decrease in phenol removal. This can be attributed to the formation of inner-sphere and outer-sphere complexes of Ni(II) through carboxylic groups and hydration on the surfaces of MWCNTs and the existence of small and compact metal cation hydration shells on metal chelates indirectly competed with phenol for sorption sites through squeezing, occupying and shielding part of the MWCNTs hydrophilic and hydrophobic sites [52].

It was also noticed that although the increase in phenol concentration from 25 to 50 mg/l resulted in small reduction in nickel removal but further increase in phenol concentration resulted in 69% reduction in nickel adsorption. These results suggest that the presence of either one of the adsorbates (Ni(II) or phenol) in the solution had a suppression effect on the other adsorbate sorption. This can be ascribed to the occurrence of a direct competition between phenol and Ni(II) for certain adsorption sites on MWCNTs [52]. Similar findings were reported by Aksu and Apmar [1] for the adsorption of phenol and nickel ions by dried activated sludge.

Comparison with other adsorbents

The sorption capacities of phenol and Ni(II) on MWCNTs were compared with other previously adsorbents reported in the literature as given in Table 5.

It was noticed that in most cases MWCNTs had higher removal efficiency for both phenol and Ni(II) in our experiments than in case of many other adsorbents, which could be attributed to its relatively larger specific surface area. Despite this, a major advantage of being effectively and conveniently separated from solution and considerably higher uptake capacity than many other adsorbents made MWCNTs a promising and excellent adsorbent to remove phenol and Ni(II) simultaneously in terms of potential application in wastewater treatment.

Real industrial effluent treatment

In order to evaluate the efficiency of MWCNTs for phenol and nickel removal from wastewater samples, an optimized procedure was used to conduct an experiment with real industrial effluents of chemicals and engineering companies in Abu-Zabal industrial area in Egypt. The removal efficiency of MWCNTs for nickel ions or phenol in wastewater samples at the optimum conditions reached up to 60% and 70%, respectively. It can be concluded that there was a slight decrease in the removal percentages of phenol and nickel by MWCNTs in real effluents compared to synthetic water. This waive in the removal efficiency can be attributed to the matrix composition of the real effluents which are likely to contain other pollutants that can compete with phenol and nickel to the MWCNTs adsorption sites.

Conclusions

The multiwalled carbon nanotubes used in the present study have been proven to have higher adsorption capacities for the removal of phenol and nickel ions from aqueous solutions. The optimum conditions for the adsorption process were found to be 300 min for contact time, a solution pH equal to 7 and adsorbent dose of 5 g/L.

The kinetics of the adsorption was described by the pseudo-second-order model and the isothermal Langmuir model was the best to describe the equilibrium of both adsorbates. The competitive adsorption results revealed that lower adsorption capacities as compared to the individual adsorption results. Comparing the present study results with the results of other adsorbents collected from literature. The desorption of both adsorbates from MWCNTs reached up to 75% using NaOH (1 M) indicating the possibility of the adsorbent reusability.

It can be concluded that the multiwalled carbon nanotubes offer a new and highly effective adsorbent that can be applied to wastewater treatment systems.

Conflict of interest

The authors have declared no conflict of interest.

Compliance with Ethics Requirements

This article does not contain any studies with human or animal subjects.

References

[1] Aksu Z, Akpınar D. Modelling of simultaneous biosorption of phenol and nickel(II) onto dried aerobic activated sludge. Sep Purif Technol 2000;21:87–99.

[2] Aksu Z, Akpinar D, Kabasakal E, Köse B. Simultaneous biosorption of phenol and nickel(II) from binary mixtures onto dried aerobic activated sludge. Process Biochem 1999;35:301–8.

[3] USEPA, Guidance manual for electroplating and metal finishing pretreatment standards; 1984.

[4] World Health Organization (WHO). Guidelines for drinking-water quality, incorporating first addendum to 3rd ed., vol. 1: Geneva: Recommendations, World Health Organization; 2006 [p. 595].

[5] Banat FA, Al-Bashir B, Al-Asheh S, Hayajneh O. Adsorption of phenol by bentonite. Environ Pollut 2000;107(3):391–8.

[6] Srivastava SK, Tyagi R, Pal N, Mohan D. Process development for the removal and recovery of substituted phenol from wastewater by a carbonaceous adsorbent developed from fertilizer waste material. J Environ Eng Divis (Am Soc Civ Eng) 1997;123:842–51.

[7] Lu C, Liu C, Su F. Sorption kinetics, thermodynamics and competition of Ni(II) from aqueous solutions onto surface oxidized carbon nanotubes. Desalination 2009;249(1):18–23.

[8] Kandaha MI, Meunier J. Removal of nickel ions from water by multi-walled carbon nanotubes. J Hazard Mater 2007;146(1–2): 283–8.

[9] Iijima S. Helical microtubules of graphic carbon. Nature 1991;354:56–8.

[10] Meyyappan M. Carbon nanotubes science and application. New York (USA): CRS Press LLC; 2005, p. 15–80.

[11] Rao GP, Lu C, Su F. Sorption of divalent metal ions from aqueous solution by carbon nanotubes: a review. Sep Purif Technol 2007;58(1):224–31.

[12] Liang P, Liu Y, Guo L, Zeng J, Lu H. Multiwalled carbon nanotubes as solid-phase extraction adsorbent for the preconcentration of trace metal ions and their determination by inductively coupled plasma atomic emission spectrometry. J Anal At Spectrom 2004;19:1489–92.

[13] Chen C, Wang X. Adsorption of Ni(II) from aqueous solution using oxidized multiwall carbon nanotubes. Ind. Eng. Chem. Res. 2006;45:9144–9.

[14] Diaz-Flores PE, López-Urías F, Terrones M, Rangel-Mendez JR. Simultaneous adsorption of Cd(II) and phenol on modified N-doped carbon nanotubes: experimental and DFT studies. J Colloid Interface Sci 2009;334:124–31.

[15] Lagergren S. Kungliga Svenska Vetenskapsakademiens Handlingar 1898;24:1–39.

[16] Ho YS, McKay G. The kinetics of sorption of basic dyes from aqueous solutions by sphagnum moss peat. Canadian J Chem Eng 1998;76(4):822–7.

[17] Weber Jr WJ, Morris JC. Kinetics of adsorption on carbon from solution. J Sanit Eng Div (Am Soc Civ) Eng 1963;89:31–60.

[18] Sheng GD, Shao DD, Ren XM, Wang XQ, Li JX, Chen YX, et al. Kinetics and thermodynamics of adsorption of ionizable aromatic compounds from aqueous solutions by as – prepared and oxidized multiwalled carbon nanotubes. J Hazard Mater 2010;178(1–3):505–16.

[19] Langmuir I. The constitution and fundamental properties of solids and liquids. J Am Chem Soc 1916;38:2221–95.

[20] Freundlich HMF. Uber die adsorption in losungen. Zeitschrift für Physikalische Chemie (Leipzig) 1906;57A:385–470.

[21] Tang WW, Zeng GM, Gong JL, Liu Y, Wang XY, Liu YY, et al. Simultaneous adsorption of atrazine and Cu(II) from wastewater by magnetic multi-walled carbon nanotubes. Chem Eng J 2012;211–212:470–8.

[22] Xu J, Lv X, Li J, Li Y, Shen L, Zhou H, et al. Simultaneous adsorption and dechlorination of 2,4-dichlorophenol by Pd/Fe nanoparticles with multi-walled carbon nanotube support. J Hazard Mater 2012;225–226:36–45.

[23] Chen C, Hu J, Shao D, Li J, Wang X. Adsorption behavior of multiwall carbon nanotube/iron oxide magnetic composites for Ni(II) and Sr(II). J Hazard Mater 2009;164(2–3):923–8.

[24] Gupta VK, Agarwal S, Saleha TA. Synthesis and characterization of alumina-coated carbon nanotubes and their application for lead removal. J Hazard Mater 2011; 185(1):17–23.

[25] Oh WC, Zhang FJ, Chen ML. Characterization and photodegradation characteristics of organic dye for Pt–titania combined multi-walled carbon nanotube composite catalysts. J Ind Eng Chem 2010;16(2):321–6.

[26] Chen ML, Oh WC. Synthesis and highly visible-induced photocatalytic activity of CNT-CdSe composite for methylene blue solution. Nanoscale Res Lett 2011;6:398. http://dx.doi.org/10.1186/1556-276X-6-398.

[27] Salam MA, Makki MSI, Abdelaal MYA. Preparation and characterization of multi-walled carbon nanotubes/chitosan nanocomposite and its application for the removal of heavy metals from aqueous solution. J Alloys Compd 2011;509(5):2582–7.

[28] Fan XJ, Li X. Preparation and magnetic property of multiwalled carbon nanotubes decorated by Fe_3O_4 nanoparticles. New Carbon Mater 2012;27:111–6.

[29] Tan X, Fang M, Cheng C, Yu S, Wang X. Counterion effects of nickel and sodium dodecylbenzene sulfonate adsorption to multiwalled carbon nanotubes in aqueous solution. Carbon 2008;46(13):1741–50.

[30] David WM, Erickson CL, Johnston CT, Defino JJ, Porter JE. Quantitative fourier transform infrared spectroscopic investigation humic substance functional group composition. Chemosphere 1999;38:2913–28.

[31] Kim SD, Kim JW, Im JS, Kim YH, Lee YS. A comparative study on properties of multi-walled carbon nanotubes (MWCNTs) modified with acids and oxyfluorination. J Fluorine Chem 2007;128(1):60–4.

[32] Gupta VK, Saleh TA. Carbon nanotubes-from research to applications. In: Stefano Bianco, editor. Syntheses of carbon nanotube-metal oxides composites; adsorption and photo-gradation, InTech; 2011. p. 295–312 [chapter 17]. http://dx.doi.org/10.5772/18009, ISBN:978-953-307-500-6, <http://www.intechopen.com>.

[33] Machado FM, Bergmann CP, Fernandes THM, Lima EC, Royer B, Calvete T, et al. Adsorption of reactive red M-2BE dye from water solutions by multi-walled carbon nanotubes and activated carbon. J Hazard Mater 2011;192:1122–31.

[34] Gupta SS, Bhattacharyya KG. Kinetics of adsorption of metal ions on inorganic materials: a review. Adv Colloid Interface Sci 2011;162:39–58.

[35] McKay G, Ho YS, Ng JCY. Biosorption of copper from wastewater: A review separation and purification methods. Sep Purif Rev 1999;28:87–125.

[36] Ho YS, McKay G. Pseudo-second-order model for sorption processes. Process Biochem 1999;34:451–65.

[37] Wu FC, Tseng RL, Juang RS. Comparative adsorption of metal and dye on flake and bead types of chitosans prepared from fishery wastes. J Hazard Mater 2000;73:63–75.

[38] Rudzinski W, Plazinski W. On the applicability of the pseudo-second-order equation to represent the kinetics of adsorption at solid/solution interfaces: a theoretical analysis based on the statistical rate theory. Adsorption 2009;15:181–92.

[39] Ho YS, McKay G. The kinetics of sorption of divalent metal ions onto sphagnum moss peat. Water Res 2000;34:35–742.

[40] Wu FC, Tseng RL, Huang SC, Juang RS. Characteristics of pseudo-second order kinetic model for liquid-phase adsorption: a mini-review. Chem Eng J 2009;151:1–9.
[41] Adolph MA, Xavier YM, Kriveshini P, Rui K. Phosphine functionalised multiwalled carbon nanotubes: a new adsorbent for the removal of nickel from aqueous solution. J Environ Sci 2012;24:1133–41.
[42] Dursun G, Ciçek H, Dursun AY. Adsorption of phenol from aqueous solution by using carbonised beet pulp. J Hazard Mater 2005;125:175–82.
[43] Juang RS, Wu FC, Tseng RL. Mechanism of adsorption of dyes and phenols from water using activated carbons prepared from plum kernels. J Colloid Interface Sci 2000;227:437–44.
[44] Hameed BH, Rahman AA. Removal of phenol from aqueous solutions by adsorption onto activated carbon prepared from biomass material. J Hazard Mater 2008;160:576–81.
[45] Bhattacharyya KG, Sarma J, Sarma A. Azadirachta indica leaf powder as a biosorbent for Ni(II) in aqueous medium. J Hazard Mater 2009;165:271–8.
[46] Rafatullaha M, Sulaiman O, Hashima R, Ahmad A. Adsorption of copper (II), chromium (III), nickel (II) and lead (II) ions from aqueous solutions by meranti sawdust. J Hazard Mater 2009;170:969–97.
[47] Mohanty K, Das D, Biswas MN. Adsorption of phenol from aqueous solutions using activated carbons prepared from Tectona grandis sawdust by $ZnCl_2$ activation. Chem Eng J 2005;115:121–31.
[48] Mohanty K, Jha M, Meikap BC, Biswas MN. Preparation and characterization of activated carbons from *Terminalia arjuna* nut with zinc chloride activation for the removal of phenol from wastewater. Ind Eng Chem Res 2005;44:4128–38.
[49] Özkaya B. Adsorption and desorption of phenol on activated carbon and a comparison of isotherm models. J Hazard Mater 2006;129:158–63.
[50] Kumar NS, Min K. Phenolic compounds biosorption onto *Schizophyllum commune* fungus: FTIR analysis, kinetics and adsorption isotherms modeling. Chem Eng J 2011;168:562–71.
[51] Rodrigues LA, Silva MLCPd, Alvarez-Mendes MO, Coutinho AdR, Thima GP. Phenol removal from aqueous solution by activated carbon produced from avocado kernel seeds. Chem Eng J 2011;174(1):49–57.
[52] Chen JY, Zhu DQ, Sun C. Effect of heavy metals on the sorption of hydrophobic organic compounds to wood charcoal. J Environ Sci Technol 2007;41:2536–41.
[53] Liao Q, Sun J, Gao L. The adsorption of resorcinol from water using multiwalled carbon nanotubes. Colloids Surf A: Physicochem Eng Asp 2008;312:160–5.
[54] Denizli A, Özkan G, Ucar M. Removal of chlorophenols from aquatic systems with dye-affinity microbeads. Sep Purif Technol 2001;24:255–62.
[55] Denizli A, Okan G, Ucar M. Dye-affinity microbeads for removal of phenols and nitrophenols from aquatic systems. J Appl Polym Sci 2002;83:2411–8.
[56] Ahmaruzzaman M, Sharma DK. Adsorption of phenols from wastewater. J Colloid Interface Sci 2005;287:14–24.
[57] Tarasevich YI. Porous structure and adsorption properties of natural porous coal. Colloids Surf A: Physicochem Eng Asp 2001;176:267–72.
[58] Vázquez I, Rodríguez-Iglesias J, Marañón E, Castrillón L, Álvarez M. Removal of residual phenols from coke wastewater by adsorption. J Hazard Mater 2007;147:395–400.
[59] Yavuz Ö, Altunkaynak Y, Güzel F. Removal of copper, nickel, cobalt and manganese from aqueous solution by kaolinite. Water Res 2003;37:948–52.
[60] Huang C, Chung YC, Liou MR. Adsorption of Cu(II) and Ni(II) by pelletized biopolymer. J Hazard Mater 1996;45:265–77.
[61] Ouki SK, Kavannagh M. Performance of natural zeolites for the treatment of mixed metal-contaminated effluents. Waste Manage Res 1997;15:383–94.
[62] Ibrahim KM, NasserEd-Deen T, Khoury H. Use of natural chabazite–phillipsite tuff in wastewater treatment from electroplating factories in Jordan. Environ Geol 2002;41:547–51.
[63] Kadirvelu K, Brasquet CF, Cloirec PL. Removal of Cu(II), Pb(II), and Ni(II) by adsorption onto activated carbon cloths. Langmuir 2000;16:8404–9.
[64] Torab-Mostaedi M, Asadollahzadeh M, Hemmati A, Khosravi A. Equilibrium, kinetic, and thermodynamic studies for biosorption of cadmium and nickel on grapefruit peel. J Taiwan Inst Chem Eng 2013;44:295–302.
[65] Gupta VK, Rastogi A, Nayak A. Biosorption of nickel onto treated alga (*Oedogonium hatei*): application of isotherm and kinetic models. J Colloid Interface Sci 2010;342:533–9.